Heliyon 10 (2024) e34204

Contents lists available at ScienceDirect

Heliyon

journal homepage: www.cell.com/heliyon

Research article

A shock-tube experimental and kinetic simulation study on the autoignition of methane at ultra-lean and lean conditions

Ziwen Zhao [a], Yeteng Wang [b], Jinchao Zhang [a], Jinhu Liang [a,**], Yang Zhang [c], Fengqi Zhao [c], Quan-De Wang [d,*]

[a] School of Environmental and Safety Engineering, North University of China, Taiyuan, 030051, PR China
[b] Hubei Institute of Aerospace Chemical Technology, Xiangfan, 441003, PR China
[c] Science and Technology on Combustion and Explosion Laboratory, Xi'an Modern Chemistry Research Institute, Xi'an, 710065, PR China
[d] Jiangsu Key Laboratory of Coal-Based Greenhouse Gas Control and Utilization, Carbon Neutrality Institute and School of Chemical Engineering, China University of Mining and Technology, Xuzhou, 221008, PR China

ARTICLE INFO

Keywords:
Methane
Ignition
Shock-tube
Detailed mechanism
Chemical kinetics

ABSTRACT

Coalbed methane represents an important kind of natural gas resource in many countries. However, the low-concentration property of coalbed methane limits its applications. To gain insight into the combustion kinetics of coalbed methane and facilitate its combustion utilization, this work reports an experimental and kinetic simulation study on the autoignition properties of methane at ultra-lean and lean conditions. A shock-tube (ST) facility is used for ignition delay time (IDT) measurements with equivalence ratios at 0.5, 0.1, and 0.05 with pressure at 2 and 10 bar under the temperature ranging from 1320 to 1850 K. The measured IDTs can be correlated into a general Arrhenius expression, and the equivalence ratio effect on IDTs is then analyzed. Seven detailed chemical kinetic mechanisms are employed to predict the IDTs and statistical error indicators are used to evaluate their performance. Detailed kinetic analysis via sensitivity and reaction path analysis is performed to uncover the kinetic differences among the seven mechanisms. It is shown that some of the reaction paths only exist in the NUIGMech1.3 mechanism, while the other detailed mechanisms do not consider them. Reaction path analysis indicates that the reactions related to O_2, OH and O species become more important compared to the reactions involving CH_3 and H radicals as the equivalence ratio decreases from lean to ultra-lean conditions. Detailed chemical kinetics analysis is also conducted to demonstrate the uncertainty of key reactions. The present work should be valuable to gain insight into the methane ignition characteristics and to facilitate kinetic mechanism optimization of methane combustion.

1. Introduction

Due to the rapid depletion of traditional fossil fuels and the continuous concerns of climate change, the usage of low-carbon, clean, and economic fuel has become an important issue for the world's energy suppliers. Natural gas accounts for more than 20 % of the world's energy consumption up to now, and shows great potential in future energy suppliers due to its increased availability with

* Corresponding author.
** Corresponding author.
E-mail addresses: jhliang@nuc.edu.cn (J. Liang), quandewang@cumt.edu.cn (Q.-D. Wang).

https://doi.org/10.1016/j.heliyon.2024.e34204
Received 22 February 2024; Received in revised form 18 June 2024; Accepted 4 July 2024
Available online 6 July 2024

relatively low-cost [1]. In addition, natural gas mainly consists of methane (CH_4) with a small number of C_2–C_3 alkanes, resulting into a very high hydrogen to carbon ratio that can lead to a significantly lower carbon dioxide (CO_2) emission compared with coal and petroleum [2]. Beside the exploration of traditional natural gas reserves, coalbed methane represents an important kind of natural gas resource in many countries that relies on coal as major resource previously, such as USA, Australia, and China [3]. In fact, during the past decades, coalbed methane is usually considered as a harmful gas for coal production due to the induction of gas explosion accident. Thus, a quantity number of coalbed methane were directly released into the atmospheres, which have aggravated the climate change process. Consequently, the exploration and usage of coalbed methane become a critical issue for both the improvement of energy efficiency and the reduction of greenhouse gas.

Coalbed methane is usually accompanied with the coal, and the concentration is usually very low, which makes it a great challenge for its combustion under ultra-lean (usually the equivalence ratio $\phi < 0.3$) and lean conditions. Thus, the improvement of utilization efficiency of low-concentration coalbed methane is an important issue for both academic and industrial research areas. Generally, the development of efficient combustors for ultra-lean and lean methane combustion requires a fundamental understanding of its combustion properties and the corresponding combustion chemistry [4]. Especially, the ignition property of fuel at ultra-lean and lean conditions is critical for the usage of coalbed methane. Although extensive experimental studies have been conducted for methane ignition covering a wide range of combustion conditions [2,5–17], very few studies are performed under ultra-lean and lean conditions. Table 1 briefly summarizes the major experimental studies on the ignition properties of methane using shock-tube (ST) and rapid compression machine (RCM), which are two major experimental facilities for the measurement of ignition delay times (IDTs). It can be seen that the studied pressure and temperature ranges were extensive, which covers the general and extreme engine conditions. The studied equivalence ratios were found to be within 0.2–6.0, which more or less covered the ultra-lean conditions. But there were only very few experimental datasets under ultra-lean conditions and the studied pressure or temperature ranges were rather limited. Further, some previous studies employed Argon gas for dilution, which deviated from the real air conditions.

The extensive experimental studies have facilitated the development of detailed chemical kinetic mechanisms to describe the combustion chemistry process of methane, and the detailed kinetic mechanism is also the foundation to couple with computational fluid dynamics for engine design. Among the various developed detailed kinetic mechanisms for methane, GRI-Mech 3.0, the first mechanism freely available on the internet to simulate natural gas [20,21] should be most successful. Recently, the Foundational Fuel Chemistry Model (FFCM-1) to predict the high-temperature combustion of H_2, H_2/CO, and CH_4 has been released to reveal the recent chemical kinetics study achievements [22]. The GRI-Mech 3.0 and FFCM-1 mechanisms are mostly related to high-temperature combustion of methane. Meanwhile, a series of other mechanisms were also developed for methane and small hydrocarbon fuels, e.g., the San Diego mechanism [23], the CRECK mechanism [24,25], and Glarborg mechanism [15,26]. In order to develop a more general detailed kinetic mechanism to reflect the state-of-the-art chemical kinetics, the widely used AramcoMech core mechanism [27] has been updated to NUIGMech1.3 [28], which has been extensively against single and blend mixtures of C_0–C_3 hydrocarbons relevant to natural gas compositions. These mechanisms have been validated for specific experimental targets, depending on the published years and the authors. But it is also worth noting that they are not comprehensively validated except for GRI-Mech 3.0 and NUIG-Mech1.3, which are developed for general purpose. However, due to the lack of extensive and systematic experimental data at ultra-lean conditions, the predictive ability of these mechanisms under these conditions is still lacking.

Based on the above considerations, the major objective of the present work is to investigate the ignition kinetics of methane under ultra-lean and lean conditions, and also to estimate the current detailed chemical kinetic mechanisms under the studied conditions. The paper is organized as follows: Section 2 details the experimental and modeling methods, Section 3 demonstrates the results and discussion, while major conclusions are summarized in Section 4.

Table 1
A brief summary of literature experiments related to CH_4 ignition studies.

Year	ϕ (Equivalence Ratio)	*P* (atm)	*T* (K)	Facility	Reference
1970	0.2–5.0	1.5–4.0	1350–1900	ST	Seery et al. [5]
1994	0.45–1.25	3–15	1300–2000	ST	Spadaccini et al. [6]
1996	0.5–4.0	9–480	1410–2040	ST	Petersen et al. [7]
1999	0.4–6	40–260	1040–1500	ST	Petersen et al. [9]
1999	0.5–6.0	35–260	1040–1600	ST	Petersen et al. [8]
2001	1.0	13–16	980–1060	RCM	Brett et al. [10]
2003	0.5	3–450	1200–1700	ST	Zhukov et al. [11]
2004	0.7–1.3	16–40	1000–1350	ST	Huang et al. [12]
2015	0.3–2.0	7–41	600–1600	ST/RCM	Burke et al. [18]
2015	0.5–2.0	1–10	1300–2000	ST	Hu et al. [13]
2016	0.5–1.0	15–80	800–1250	RCM	Hashemi et al. [15]
2016	0.5–2.0	3.75–22	900–2000	ST/RCM	Leschevich et al. [16]
2016	0.5–2	9.9–39.5	1400–2000	ST	Merhubi et al. [14]
2020	0.25–1.0	9.9	880–1500	ST	Merkel et al. [17]
2020	0.2–5.0	10–55	1450–1850	ST	Shao et al. [19]

2. Experimental and modeling methods

2.1. Shock-tube experiment

The ignition kinetics of methane under ultra-lean and lean conditions are studied using a ST facility at North University of China, which has been detailed and validated in previous studies [29–32]. A short description of the ST is given here for simplicity. The ST is composed of a low-pressure section with 6.8 m long, a high-pressure section with 3 m long, and a 0.3 m double-membrane section between the low-pressure and high-pressure sections. The inner diameter of the ST is 0.1 m. Before experiments, the fuel/air mixture is prepared in a gas distribution tank according to Dalton's law of partial pressures and has been static for more than 12 h to obtain homogenous mixture. The incident shock velocity is measured by using five piezoelectric transducers (PCB113B26) at the low-pressure section sidewall. The tailored interface method [33] is used when the IDTs is longer than 1 ms during the experimental period. The IDT is defined as the time interval between the pressure increase caused by the arrival of the incident shock at the endwall and the maximum rate of increase of the pressure signal, as shown in Fig. 1(a). For the ultra-lean condition, the pressure rise rate (dp/dt) is small and the IDT can't be measured. The pressure trace and the OH* emission signal are used together to define the IDT. The IDT defined as the time interval between the pressure increase caused by the arrival of the incident shock at the endwall and the maximum rate of increase of the first OH* emission signal, as shown in the below Fig. 1(b).

The uncertainty of the IDTs in the ST experiment is mainly attributed to the uncertainty of the temperature behind the reflected shock wave [34], which is caused by the error in the measurement of the incident shock velocity. Specifically, uncertainty of the distance between the adjacent pressure transducers and the times recorded using the oscilloscope, at which the shock passes, is the main factor that influences the accuracy of the incident shock velocity. In the present ST experiment, the uncertainty in the time interval is determined from the signals recorded by 5 × PCB 113B26 pressure transducers using the oscilloscope. This uncertainty is estimated to be 1 μs, which is related to the sampling rate of the pressure transducers and the oscilloscope. The uncertainty in the distance between the adjacent pressure transducers is estimated to be ±0.1 mm, which is mainly due to the shock front thickness and the diameter of the sensing area of the pressure transducers. Based on Petersen et al. [35] and Mohammadreza et al. [34], this could lead to a maximum uncertainty of ±20 K for the temperature after the reflected shock. The other factors including pressure, equivalence ratio and even diluent concentration together with the facility effect can also affect the uncertainty of IDTs. Consequently, the uncertainty of the IDTs is not a constant parameter. Through previous comparisons with other related facilities, the IDTs via the present ST facility are in good agreement with other ST facilities [29,35,36], indicating the uncertainty should be consistent. Together with detailed analysis from Mohammadreza et al. [34] on the above factors, the overall uncertainty of the present ST experiment can be controlled within 20 %. For the ultra-lean conditions, it has been shown that the uncertainty of IDTs from ST is consistent with traditional studied combustion conditions [37].

The fuel/air mixture studied in the present work is fuel/air with a ratio of 3.76 of N_2/O_2. For stoichiometric combustion of CH_4, the stoichiometric relationship is $CH_4 + 2(O_2 + 3.76N_2) = CO_2 + 2H_2O + 7.52N_2$. An equivalence ratio is fuel-air-ratio/(fuel-air-ratio) stoichiometric. Consequently, the equivalence ratio can be derived through the official definition as ϕ = real(CH_4: Air)/stoichiometric(CH_4: Air). Table 2 lists the specific reactant mixtures together with the studied pressure and temperature conditions. The studied equivalence ratios are 0.05, 0.1, and 0.5. The driving gas is Helium with purity of 99.999 %. The purity of oxygen and nitrogen is also 99.999 %, while the purity of methane is 99.99 %.

2.2. Kinetic simulation methods

As shown previously, several detailed kinetic mechanisms have been developed for methane due to importance for the development of detailed mechanisms of large fuels induced by the hierarchical nature of combustion kinetic mechanisms. In this work, several typical mechanisms for methane are employed for kinetic simulation to estimate their performance. The adopted detailed kinetic

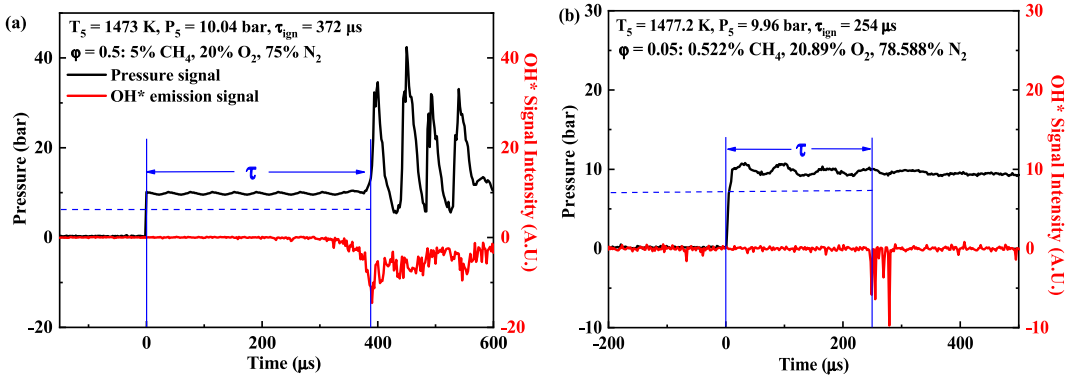

Fig. 1. Typical pressure and OH* emission signals for the definition of the IDTs during the ignition process of methane at lean condition (a) and at ultra-lean condition (b).

Table 2
Composition of the reactant mixtures (mol fraction) and detailed conditions in ST experiment.

ϕ	CH_4(%)	O_2(%)	N_2(%)	P_5 (bar)	T_5 (K)
0.05	0.522	20.89	78.588	2, 10	1350–1850
0.1	1.039	20.782	78.179	2, 10	1320–1850
0.5	5.000	20	75	2, 10	1340–1850

mechanisms include GRI-Mech 3.0 [20], FFCM-1 [22], the mechanism developed by Glarborg et al. (denoted as Glarborg mech) [26], AramcoMech 3.0 [38], Polimi mechanism [25], NUIGMech1.3 mechanism [28], and the OXYMECH2.0 mechanism for lean combustion of small alkane molecules [39]. The related references and the corresponding species and reactions in the detailed mechanism are listed in Table 3. To speed up simulation of the experimental results and the following sensitivity analysis, the NUIGMech1.3 containing 2998 species and 12761 species has been reduced to a skeletal mechanism with 106 species and 912 reactions as shown in Table 3 using a series of directed relation graph-based methods [40–42]. The simulation results for the detailed and reduced models are nearly identical, and reaction path analysis indicates that all the important species/reactions are retained in the reduced mechanism. Kinetic simulation of the ST facility for IDTs is performed by using a closed homogeneous batch reactor at constant volume, which is confirmed to be efficient to capture the ignition kinetics under the studied conditions [43,44]. The Cantera software [45] is used for all simulations. The IDT during the kinetic simulation process is defined as the extrapolation of the maximum pressure gradient (dp/dt) to the zero point, which is consistent with experimental definitions.

3. Results and discussion

3.1. IDTs of CH_4 at lean and ultra-lean conditions

To demonstrate the accuracy of the experimental results, the IDTs derived in this work at equivalence ratio of 0.5 and 10 bar are compared with those obtained by Burke et al. [18]. The fuel concentration in Burke's experiment at this condition is 0.499, which is very close to that in this work. From Fig. 2, the present measurements are in good agreement with the results except for the point at the highest temperature condition. Through a linear fitting analysis, it is shown that the present results demonstrate a better Arrhenius expression of the IDTs compared with that Burke et al. [18], confirming the present results could be much reliable at high temperature conditions. In addition, Fig. 2 also indicates that the present work further extends the combustion conditions of IDTs for methane, which should be valuable for mechanism validation and optimization.

Fig. 3 displays the concrete effects from pressure, temperature, and equivalence ratio on the IDTs of methane under air ($O_2/N_2 = 1/3.76$) conditions using the present data and literature values [18]. Generally, the temperature demonstrates the largest effect on the IDTs, which exhibits an exponential relationship similar to all other hydrocarbons. The pressure shows a promotion effect on the IDTs of methane, meaning that the IDTs can be decreased as pressure increases. From Fig. 3(a), it can be seen that the IDTs of methane decrease as equivalence ratio decreases from 0.5 to 0.1 at both 2 and 10 bar, and this trend is more obvious at low pressure condition (2 bar). However, further decreasing of the equivalence ratio from 0.1 to 0.05 does not demonstrate obvious effect on the measured IDTs. In combination with the results by Burke et al. [18], the effect on IDTs of methane from equivalence ratio is smaller compared with that from pressure and temperature, and the IDTs gradually decrease as equivalence ratio decreases under the studied combustion temperature and pressure ranges, which shows an opposite trend compared with the IDTs of methane under low temperature conditions revealed from RCM measurements [18]. The effect from equivalence ratio demonstrates the effect from fuel concentration and chain-branching reactions on the IDTs, which has been discussed by Bugler et al. [46].

To further demonstrate the effects from temperature, pressure, and equivalence ratios on the IDTs, the general Arrhenius expression is used to fit the measured IDTs of methane under lean and ultra-lean conditions in this work and the combined IDTs under equivalence ratio conditions from 0.05 to 2.0 with literature values under the similar pressure and dilution conditions. The adjusted R-squared, a modified version of R-squared that adjusts for the number of predictors in a regression model is used to check the accuracy of the fitted expressions. The closer the value is to 1, the better the fitting results is. In the present work, the values for the two expressions are 0.98 and 0.97, respectively, revealing the fitting results are reasonable. Fig. 4 shows the fitted results together with the Arrhenius expressions. It can be seen that the fitted results demonstrate very good Arrhenius tendency and only very fewer points slightly deviate from the fitted line. From Fig. 4(a) and (b), the fitted activation energy for equivalence ratios ranging from 0.05 to 0.5

Table 3
Overview of kinetic mechanisms available in the current literature.

Mechanism	Year	Number of species	Number of reactions
GRI-Mech 3.0	1999	53	325
AramcoMech3.0	2015	581	3037
FFCM-1	2016	38	291
Glarborg mechanism	2018	151	1363
Polimi mechanism	2019	151	2335
OXYMECH2.0	2020	495	2825
NUIGMech1.3	2022	106	912

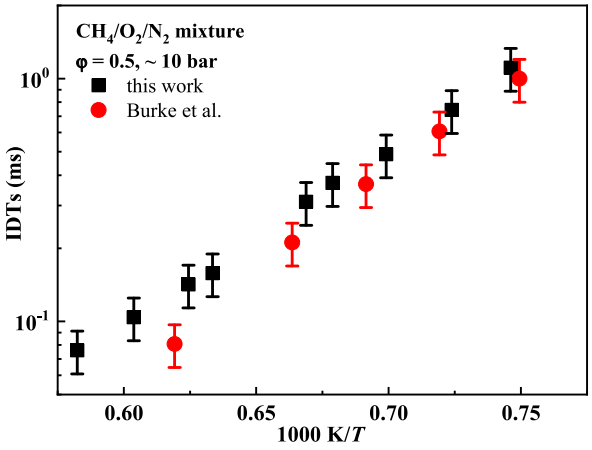

Fig. 2. Comparisons of the present experimental results with literature data by Burke et al. [18] at equivalence ratio of 0.5 and 10 bar.

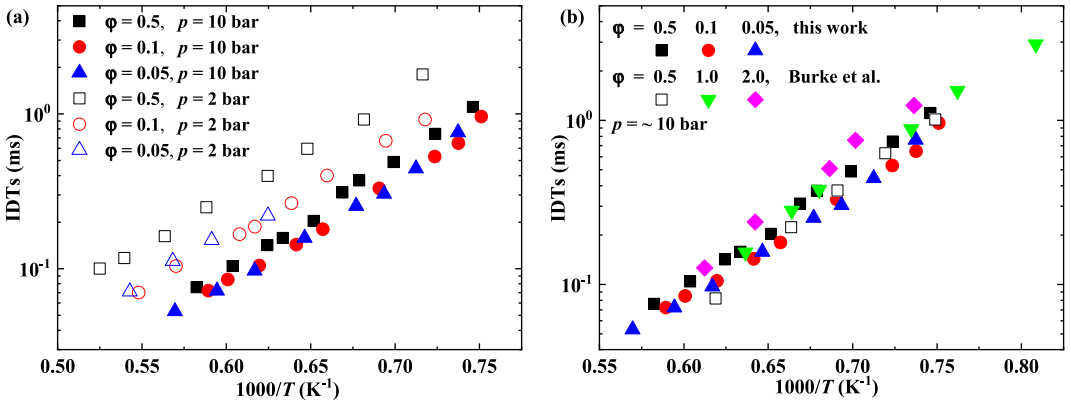

Fig. 3. (a) Effect of pressure, equivalence ration, and temperature effect on IDTs in this work; (b) Effect of equivalence ratio effect on IDTs at ~ 10 bar from data in this work and by Burke et al. [18].

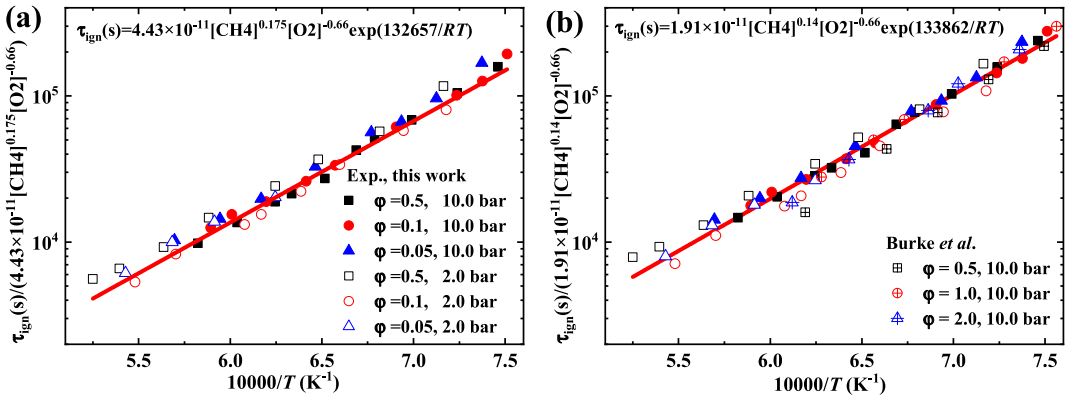

Fig. 4. Data fitting of the IDTs of methane under air conditions according to the Arrhenius expression: (a) Fitting of the present experimental results; (b) Fitting of the present experimental results together with the results by Burke et al. [18].

is 31705.78 cal/mol, and it is smaller than that with a value of 31993.79 cal/mol for equivalence ratios from 0.05 to 2.0 by adding fuel rich-condition results, indicating that the methane at fuel-lean conditions tends to be easier to ignite at the studied pressure and temperature conditions. The results shown in Fig. 3 also reveal this phenomenon. As shown by the exponential factor of oxygen, the fitted results are identical with a value of −0.66, revealing the negative effect of oxygen concentration on IDTs of methane due to the

equivalence ratio shifting from rich to lean as oxygen concentration increases. On the other hand, the fuel concentration demonstrates a positive effect on the IDTs, and the effect slightly decreases as the fitted data set increases. Overall, the good correlation of the IDTs of methane in Arrhenius expressions can be helpful to identify the experimental results with large uncertainty and should be valuable for the quick estimation of IDTs in complex engine design processes.

3.2. Evaluation of detailed kinetic mechanisms

Fig. 5 shows the predicted IDTs of methane under different conditions measured in this work. Generally, the employed mechanisms can well predict the measured IDTs within the experimental uncertainty except for a few experimental results at extremely high temperature conditions. It is also worth noting that at extremely high temperature conditions, the uncertainty tends to be larger due to the very short ignition process. Specifically, all the mechanisms tend to predict faster IDTs at high-temperature regions above 1600 K, while the employed mechanisms demonstrate different performance under temperature below 1600 K. At equivalence ratio of 0.5 and pressure of 10 bar, the employed mechanisms generally demonstrate good performance except for the GRI-Mech 3.0 mechanism with

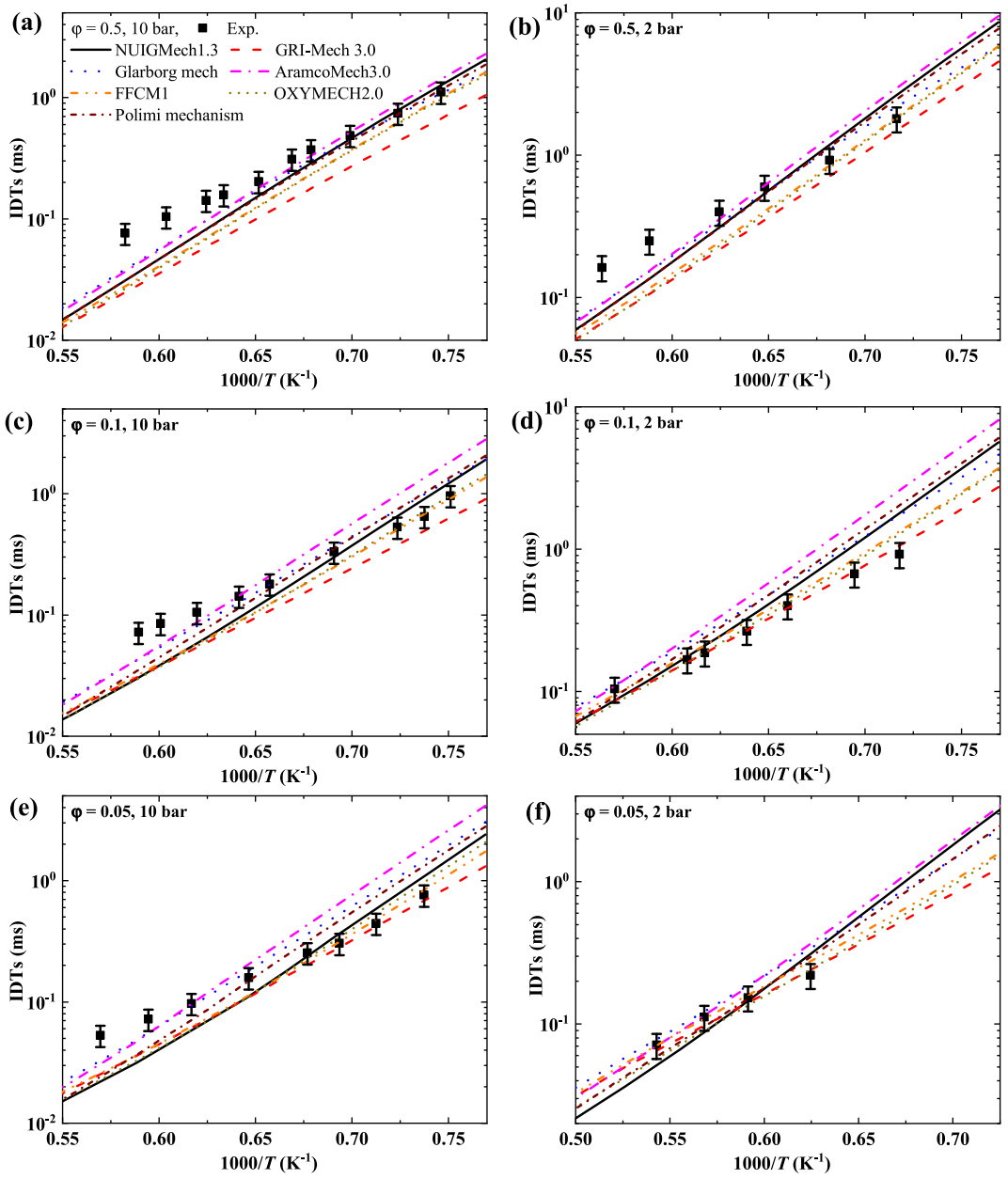

Fig. 5. The predicted IDTs of methane under different conditions in this work using the employed seven kinetic mechanisms.

large deviations at temperature lower than 1600 K. As equivalence ratio shifts from 0.5 to 0.1 and 0.05, the FFCM-1, GRI-Mech 3.0, and NUIGMech1.3 mechanisms tend to show slightly better performance. At low pressure conditions, i.e., 2 bar, it can be seen that the GRI-Mech 3.0 mechanism demonstrates the best performance at equivalence ratio of 0.1 and 0.05. At equivalence ratio of 0.5 and pressure of 2 bar, all the mechanisms exhibit very similar performance and the prediction accuracy is strongly dependent on the specific experimental conditions.

In order to quantitatively evaluate the prediction accuracy of the employed seven kinetic mechanisms, statistical error analysis is performed by computing the following four error indicators, i.e., the standard deviation (σ), the mean absolute deviation (MAD), the mean square error (MSE), and the mean absolute percentage error (MAPE) through equations (1)–(4) between the predicted IDTs (τ_{model}) and the experimental measurements (τ_{Exp}) [47,48]:

$$\mathrm{MAD} = \frac{1}{n}\sum \left|\tau_{model} - \tau_{Exp}\right| \tag{1}$$

$$\sigma = \sqrt{\frac{\sum \left(\tau_{model} - \tau_{Exp}\right)^2}{n}} \tag{2}$$

$$\mathrm{MSE} = \frac{1}{n}\sum \left(\tau_{model} - \tau_{Exp}\right)^2 \tag{3}$$

$$\mathrm{MAPE} = \frac{1}{n}\sum \frac{\left|\tau_{model} - \tau_{Exp}\right|}{\tau_{Exp}} \tag{4}$$

The statistical error analysis results are explicitly shown in Fig. 6. As shown in Fig. 6, the foure indicators reveal that the FFCM-1 and GRI-Mech 3.0 mechanisms exhibit the best performance among the analyzed seven kinetic mechanisms, because the major targets of the two mechanisms were developed for methane combustion and literature IDTs data was employed for mechanism optimization [20,22]. Follows are the OXYMECH2.0, Glarborg and NUIGMech1.3 mechanisms, which shows similar performance. In fact, these mechanisms show good performance at high pressure conditions due to the recent engine performance teowarding to high-pressure conditions. The old version of NUIGMech1.3, i.e., AramcoMech3.0 mechanism, shows the largest error indicators, mainly because it was focused on small alkenes molecules as the targets [27].

3.3. Sensitivity analysis and reaction path analysis

Fig. 7 explicitly shows the brute-force sensitivity analysis results using FFCM-1 and NUIGMech1.3 mechanisms at 1400 and 1600 K with equivalence ratio of 0.05 and pressure of 10 bar. Brute-force sensitivity analysis is conducted by changing one reaction rate constant with a factor of 2 to check its impact on the predicted IDT, and this process is repeated until all reactions are considered. The GRI-Mech 3.0 and Glarborg mechanisms are also employed for sensitivity analysis. However, it is demonstrated that the sensitivity results are very similar among the different mechanisms. Only slight deviations of the computed sensitivity coefficients are observed. From Fig. 7, the reactions $CH_3 + HO_2 = CH_3O + OH$, $CH_3 + O_2 = CH_3O + O$, and $H + O_2 = O + OH$ exhibit the largest negative sensitivity coefficients in most cases due to the chain-branching nature of the last two reactions and also the consumption of low-reactivity CH_3 radical by HO_2 and O_2. On the contrary, the radical recombination reactions including $2CH_3(+M) = C_2H_6(+M)$ and $CH_3 + OH = CH_3OH$ and the chain-termination reaction $OH + HO_2 = H_2O + O_2$ show large positive sensitivity coefficients. Besides, it is

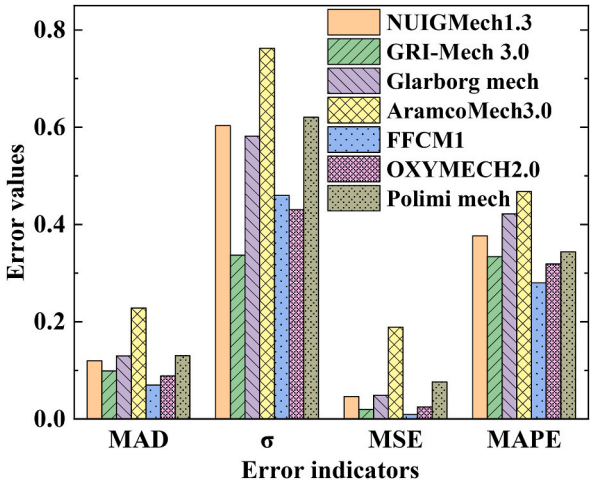

Fig. 6. Statistical error analysis of the seven mechanisms in the prediction of the measured IDTs of methane in this work.

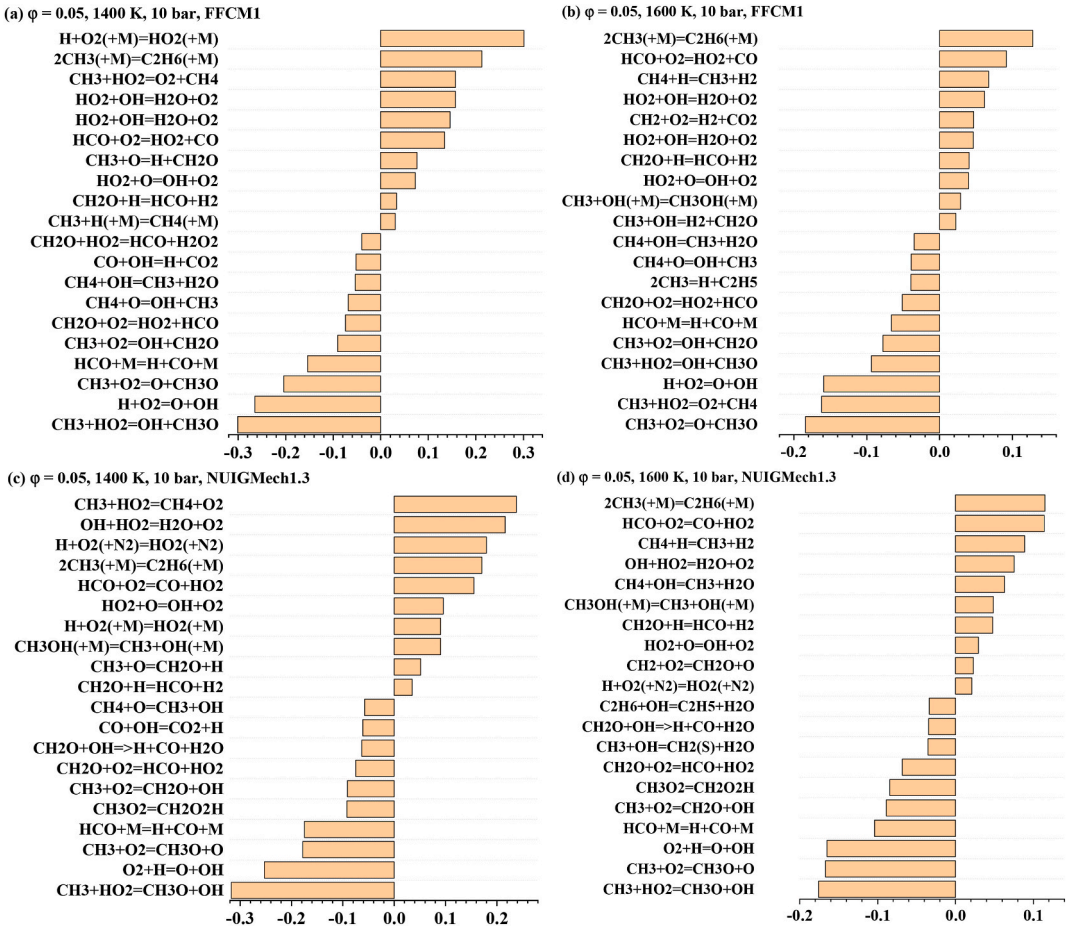

Fig. 7. The top 10 reactions with positive and negative sensitivity coefficients that affects the IDTs of methane at $\phi = 0.05$, $p = 10$ bar, and $T = 1400$ and 1600 K conditions from brute-force sensitivity analysis.

found that as temperature increases, the reactions involving the consumption of H radical tend to slow the system reactivity due to the large participation of H radical at high temperature combustion conditions. Specifically, the reaction $CH_4 + H{=}CH_3 + H_2$ demonstrates very large positive effect on IDTs, and this trend is observed from all the considered seven detailed mechanisms. The importance of this reaction is mainly contributed to the consumption of reactive H radical and the formation of CH_3 radical under high temperature combustion conditions. Considering the impact of this reaction, the increasement of the rate constant of this reaction by a factor of about 2~3 can significantly improve the model performance of NUIGMech1.3 at temperature above 1600 K. A detailed discussion of the kinetics of major reactions is performed later. Through detail insight into the detailed chemical kinetics of the seven mechanisms, a critical difference is the inclusion of $CH_3O_2{=}CH_2OOH$ in the NUIGMech1.3 mechanism, which is not considered in the other six detailed mechanisms. From Fig. 7, this reaction is also one of the most important reactions with negative sensitivity coefficients. After removing this reaction in the NUIGMech1.3 mechanism, it is found that the predicted IDTs tend to be larger than the original one, especially at low temperature conditions. However, the reaction and its rate constants remain to be solved [49–51]. To sum up, the sensitivity analysis results using the seven detailed mechanism in most cases are very similar, and the biggest difference between NUIGMech1.3 mechanism and the other 6 mechanisms is the inclusion of the reaction $CH_3O_2{=}CH_2OOH$. Thus, the different prediction performance is mostly induced by the different rate constants employed in the detailed mechanisms.

To further show the chemical kinetics of methane ignition at the studied conditions, Fig. 8 demonstrates the dominant reaction path of methane at fuel consumption of 50 % via rate-of-production (ROP) analysis during ignition processes at temperatures of 1400 and 1600 K, equivalence ratio of 0.5 and 0.05 with pressure of 10 bar. Considering the similarity of the mechanisms, Fig. 8 demonstrates the results using the NUIGMech1.3 and FFCM-1 mechanisms. Compared with the reaction path analysis using the two mechanisms, it can be seen that the dominant reaction path and major reactions to the oxidation path of methane are nearly identical except the reaction path of CH_3. To be more specific, it is shown that at fuel ultra-lean conditions, the reaction of CH_3 with O_2 to the formation of CH_3O_2 plays an important role in the NUIGMech1.3 mechanism. The major following reaction path of CH_3O_2 is transformed to CH_2OOH radical via isomerization reaction, which is not considered in the other detailed mechanisms. However, the reaction path of CH_3 with O_2 to CH_3O_2 and then to CH_2OOH radical mainly occurs at ultra-lean conditions probably due to the high O_2 concentrations. Both the NUIGMech1.3 and FFCM-1 mechanisms show that the initial oxidation of methane starts from the abstraction reactions by OH

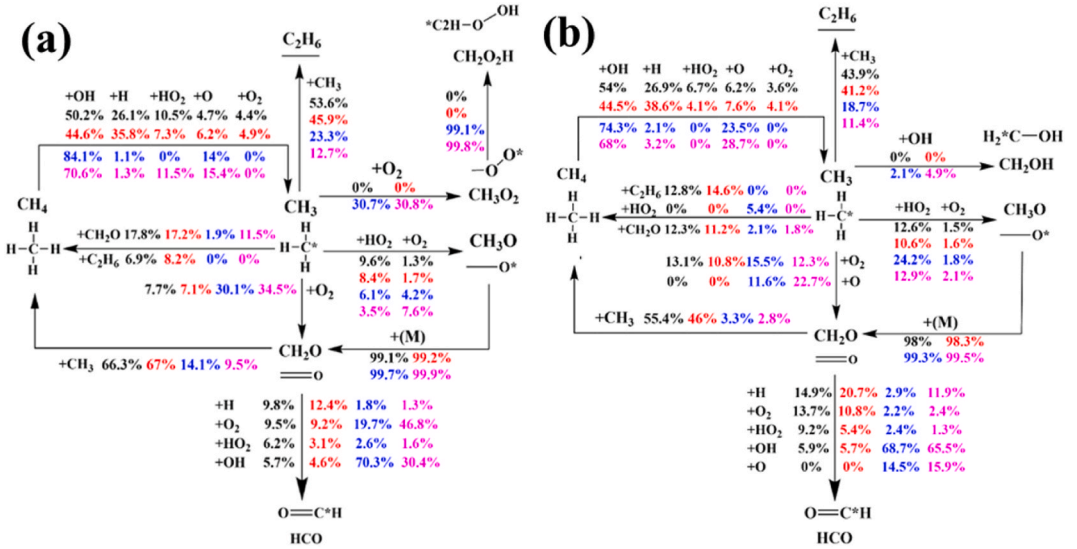

Fig. 8. Reaction path analysis using the NUIGMech1.3 mechanism (a) and FFCM-1 mechanism (b) during ignition process when the fuel is consumed by 50 %. The numbers in black and red color represent the reaction contributions to the consumption of species at temperatures of 1400 and 1600 K with equivalence ratio of 0.5 and pressure of 10 bar, while the numbers in blue, and purple color represent that at temperatures of 1400 and 1600 K with equivalence ratio of 0.05 and pressure of 10 bar. (For interpretation of the references to color in this figure legend, the reader is referred to the Web version of this article.)

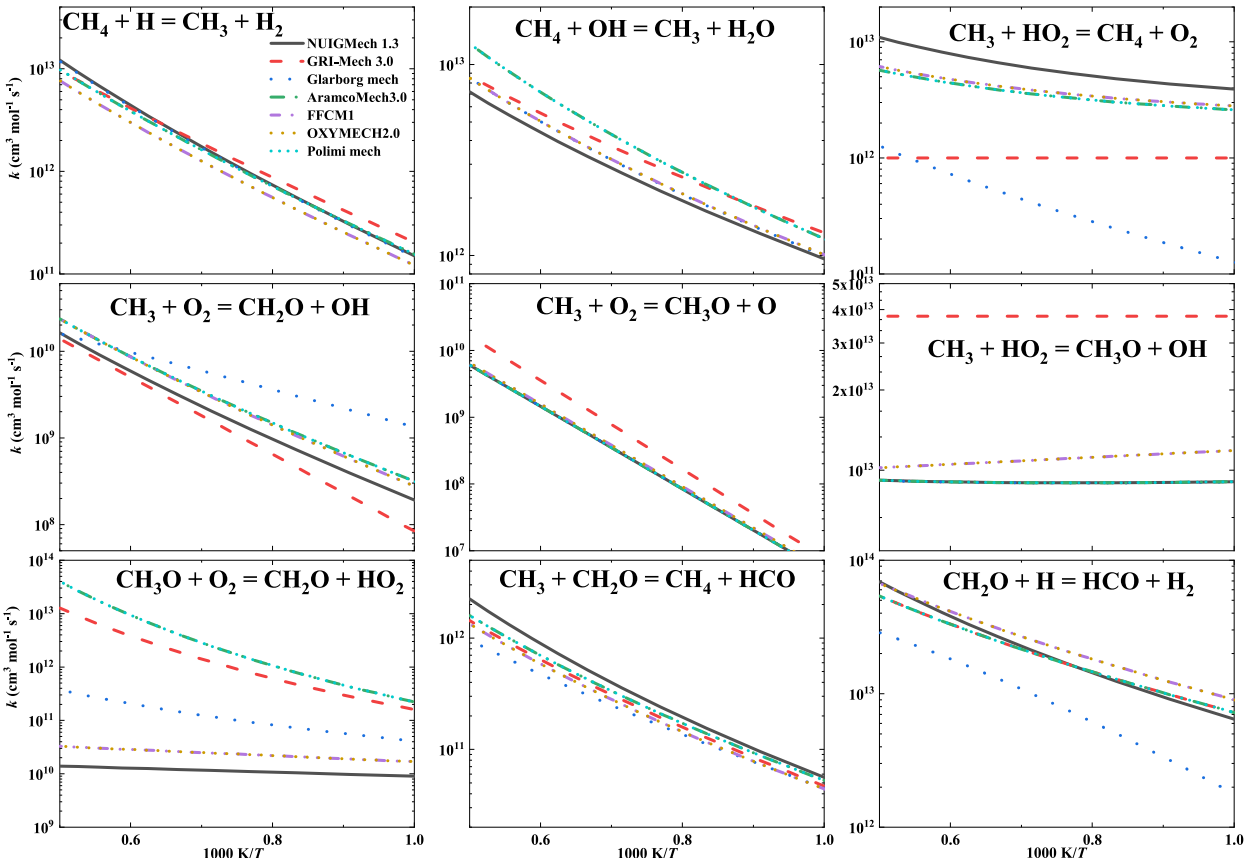

Fig. 9. Rate constants of major reactions affecting the ignition of methane employed in the different detailed kinetic mechanisms.

and H radicals. However, the contributions from the abstraction reactions by different radicals change significantly at lean and ultra-lean conditions. The contribution from the abstraction reaction by OH radical increases significantly, while that by H radical decreases as the equivalence ratio decreases from 0.5 to 0.05. In addition, the abstraction reaction by O radical also increases as the equivalence ratio decreases. The following reaction path of CH_3 radical is mainly towards to the formation of ethane (C_2H_6), CH_2O and CH_3O species. For the radical recombination reaction of CH_3 to form C_2H_6, it can be seen that the contribution of this reaction decreases as the equivalence ratio decreases, which should be mainly induced by the low concentration of CH_3 radical at ultra-lean conditions. The formation of CH_3O radical is mainly via the reaction of CH_3 with HO_2 and O_2 species, and the contributions do not show large changes as the combustion condition changes. The formed CH_3O radical is subsequently converted into CH_2O by nearly 100 % through the decomposition reaction, i.e., $CH_3O(+M) = CH_2O + H(+M)$. The reaction of CH_3 with O_2 to the formation of CH_2O represents another major consumption path of CH_3, and this reaction becomes important at ultra-lean conditions from the NUIGMech1.3 mechanism, which should be induced by the increasement of the O_2 concentration. The following reaction path of CH_2O is mostly controlled by the reactions with CH_3, H, O, OH radicals to the formation of HCO, which subsequently converts to the final products, i.e., CO and CO_2. It can be seen that the reactions of CH_2O with CH_3 and H becomes less important, while the reactions of CH_2O with O_2 and OH become more important as the equivalence ratio decreases, which could also be induced by the different fuel/O_2 ratios in the initial reactant mixtures defined via the equivalence ratio. To sum up, due to the very different fuel/O_2 ratios at lean and ultra-lean conditions, the reaction path of methane ignition is different. The reactions related to CH_3 and H radical become less important compared with the reactions involving O_2 and OH species as the equivalence ratio decreases due to the concentration changes of different species, i.e., the contribution of CH_3 radical recombination reaction to C_2H_6 decrease by more than a factor of 2, while the reaction of CH_3 with O_2 increases by a factor of 4 as the equivalence ratios change from 0.5 to 0.05.

3.4. Implications for chemical kinetics of methane ignition

From sensitivity analysis and reaction path analysis, the ignition process of methane is mainly controlled via a small number of reactions, and the rate constants of these reactions obviously show large impact on the predicted IDTs. To gain insight into the difference among the considered detailed mechanisms and obtain useful information for further mechanism optimization, Fig. 9 compares the rate constants of major reactions as a function of temperature (from 1000 to 2000 K) employed in the detailed mechanisms. It can be seen that although the predicted IDTs can generally reflect the variations across different combustion conditions, i.e., pressure, temperature, and equivalence ratio, the employed rate constants of the key reactions are different. For the initial abstraction reaction of methane with H radical, the rate constants as a function of temperature in different mechanisms are very similar, however, the absolute values remain different. As shown from sensitivity analysis, a small variation of this reaction rate constant can exhibit large effect due to the large sensitivity coefficient. The rate constants over the temperature range 928–1697 K derived by Sutherland et al. [52] using the laser photolysis shock-tube technique coupled with H-atom atomic resonance absorption spectrometry have been used in the recently developed mechanisms, i.e., NUIGMech1.3 and Glarborg mechanisms. The optimized rate constants in GRIMech-3.0 and FFCM-1 mechanisms do not show large deviations as shown in Fig. 9. For the reaction $CH_4 + OH{=}CH_3 + H_2O$, the rate constants are nearly identical except that used in the GRI-Mech 3.0 and AramcoMech3.0 mechanisms. In fact, the rate constants employed in NUIGMech1.3 were from experimental measurement using reflected shock-tube technique with multi-pass absorption spectrometric detection [53], and it was multiplied by a factor of 1.5 in the AramcoMech3.0. Overall, the rate constants of the above two reactions contributed to major consumption of methane do not exhibit large uncertainty.

For the reaction $CH_3 + HO_2{=}CH_4 + O_2$, large uncertainty can be observed due to the very large different reaction rate constants. As shown in Fig. 9, this reaction is also competitive with the reaction path to $CH_3O + OH$, which is chain propagation in nature due to the formation of highly reactive OH radical from the much less reactive CH_3 and HO_2 radicals. Although theoretical and experimental studies have been performed on the reaction $CH_3 + HO_2{=}CH_4 + O_2$ or its reverse reaction, the rate constants employed in the detailed mechanisms are rather different. The GRI-Mech 3.0 employed a constant value of 1.0×10^{12} cm^3 mol^{-1} s^{-1} as the rate constant, which lies between the Glarborg mechanism and the other mechanisms. The reaction rate constants of $CH_4 + O_2{=}CH_3 + HO_2$ by Srinivasan et al. [54] is employed in the Glarborg mechanism, however, the reverse rate constants tend to low than the other reactions. The theoretical results by Zhu et al. [55] are used in the NUIGMech1.3 mechanism, and they are generally larger than the other rate constants over the considered temperature ranges. The theoretical results by Jasper et al. [56] are employed in the other mechanisms, and the results are supported by experimental studies by Hong et al. [57]. It can be seen that the rate constants are similar to that by Zhu et al. [55], and only slight deviations are observed compared with the rate constants used in GRI-Mech 3.0 and the derived reverse rate constants.

For the reaction of CH_3 with O_2, the two reaction channels to $CH_2O + OH$ and $CH_3O + O$ both reveal negative sensitivity coefficients as shown from Fig. 7, which mean that they can increase the system reactivity when the rate constants are increased due to the formation of reactive radicals from the reactants. From Fig. 9, the two reaction rate constants are generally similar except those in the GRI-Mech 3.0 and Glarborg mechanisms. From Fig. 9, another reaction with large uncertainty of the rate constants is $CH_3O + O_2{=}CH_2O + HO_2$. Fortunately, this reaction demonstrates smaller sensitivity coefficients and less reaction contributions via sensitivity analysis and ROP analysis. Beside these biomolecular reactions, pressure-dependent radical recombination reaction, i.e., $2CH_3(+M) = C_2H_6(+M)$ is also critical for methane ignition, which has been discussed in detail recently by Kashif et al. [58], and the uncertainty of this reaction tends to be reduced via extensive research in recent years.

4. Conclusions

This work reports an experimental and kinetic simulation study on lean and ultra-lean methane ignition relevant to coalbed methane utilization. Shock-tube is employed to measure the IDTs covering a wide range of conditions, i.e., equivalence ratios at 0.5, 0.1, and 0.05, pressure at 2 and 10 bar, and temperature ranging from 1320 to 1850 K. Kinetic simulation is performed employed seven detailed kinetic mechanisms. The major results can be summarized as follows:

(1) The IDTs of methane can be decreased as pressure and temperature increase in the studied combustion conditions, and it is also decreased as equivalence ratio decreases from 0.5 to 0.1. But further decreasing of the equivalence ratio from 0.1 to 0.05 does not demonstrate obvious effect on the measured IDTs.
(2) The measured IDTs can be correlated into good Arrhenius expressions, and the fitted activation energies reveal that the methane at fuel-lean conditions tends to be easier to ignite at the studied pressure and temperature conditions.
(3) The seven detailed mechanisms can predict the variations of IDTs as a function of pressure, temperature and equivalence ratio. However, the prediction accuracy strongly depends on the combustion conditions. Statistical error analysis indicates the specially optimized mechanisms for methane including GRI-Mech3.0 and FFCM-1 exhibit better performance, and the recently developed comprehensive NUIGMech1.3 mechanism also show good performance, especially at high pressure conditions.
(4) From reaction path analysis, the reactions involving O, OH, and O_2 species tend to be more important compared with that with H and CH_3 radicals as equivalence ratio decreases due to the existence of more oxygenated species at fuel ultra-lean conditions.
(5) Reaction path for methane oxidation in different detailed mechanism is different. The reaction CH_3O_2═CH_2OOH via isomerization is only considered in the comprehensive NUIGMech1.3 mechanism. Detailed chemical kinetic analysis indicates that large uncertainties of the rate constants still exist for the reactions including CH_3O_2═CH_2OOH, $CH_3 + HO_2$═$CH_4 + O_2$ (or the reverse reaction), $CH_3 + HO_2$═$CH_3O + OH$, $CH_3O + O_2$═$CH_2O + HO_2$, $2CH_3$═$C_2H_5 + H$, and $HCO + O_2$═$CO + HO_2$. Overall, the present work should be valuable for coalbed methane combustion utilization and further optimization of detailed mechanism.

Data availability statement

All the data used to support the findings of this study are included within the article and the supplementary materials.

Ethics declarations

Not Applicable.

CRediT authorship contribution statement

Ziwen Zhao: Writing – original draft, Formal analysis, Data curation. **Yeteng Wang:** Formal analysis, Data curation. **Jinchao Zhang:** Formal analysis. **Jinhu Liang:** Writing – review & editing, Resources, Formal analysis, Data curation. **Yang Zhang:** Formal analysis. **Fengqi Zhao:** Data curation. **Quan-De Wang:** Writing – review & editing, Formal analysis, Data curation.

Declaration of competing interest

We declare that we have no financial and personal relationship with other people or organization that can inappropriately influence our work, there is no professional or other personal interest of any nature or kind in any product, service and/or company that could be constructed as influencing the position presented in, or the review of, the paper entitled.

Acknowledgments

We are grateful to the financial foundations from the Natural Science Foundation of China (Nos. 12172335, U2133215 and 22205178), the Scientific Activities of Selected Returned Overseas Professionals in Shanxi Province (No. 20230014), and the Key Laboratory Fund of the Ministry of Public Security of the People's Republic of China (No. 2023FMKFKT01). The authors also thank Dr. Yang Hu from Key Laboratory of Toxic and Harmful Gas Monitoring and Early Warning, Ministry of Emergency Management for helpful discussion and valuable comments on the manuscript.

Appendix A. Supplementary data

Supplementary data to this article can be found online at https://doi.org/10.1016/j.heliyon.2024.e34204.

References

[1] M.A. Mac Kinnon, J. Brouwer, S. Samuelsen, The role of natural gas and its infrastructure in mitigating greenhouse gas emissions, improving regional air quality, and renewable resource integration, Prog. Energy Combust. Sci. 64 (2018) 62–92.
[2] J.M. Mehta, W. Wang, K. Brezinsky, Shock tube study of natural gas oxidation at propulsion relevant conditions, Proc. Combust. Inst. 39 (2023) 39–48.
[3] Z. Huang, C. Sednek, M.A. Urynowicz, H. Guo, Q. Wang, P. Fallgren, S. Jin, Y. Jin, U. Igwe, S. Li, Low carbon renewable natural gas production from coalbeds and implications for carbon capture and storage, Nat. Commun. 8 (2017) 568.
[4] H.J. Curran, Developing detailed chemical kinetic mechanisms for fuel combustion, Proc. Combust. Inst. 37 (2019) 57–81.
[5] D.J. Seery, C.T. Bowman, An experimental and analytical study of methane oxidation behind shock waves, Combust. Flame 14 (1970) 37–47.
[6] L.J. Spadaccini, M.B. Colket, Ignition delay characteristics of methane fuels, Prog. Energy Combust. Sci. 20 (1994) 431–460.
[7] E.L. Petersen, M. Röhrig, D.F. Davidson, R.K. Hanson, C.T. Bowman, High-pressure methane oxidation behind reflected shock waves, Symp. (Int.) Combust. 26 (1996) 799–806.
[8] E.L. Petersen, D.F. Davidson, R.K. Hanson, Ignition delay times of ram accelerator CH_4/O_2/diluent mixtures, J. Propul. Power 15 (1999) 82–91.
[9] E.L. Petersen, D.F. Davidson, R.K. Hanson, Kinetics modeling of shock-induced ignition in low-dilution CH4/O2 mixtures at high pressures and intermediate temperatures, Combust. Flame 117 (1999) 272–290.
[10] L. Brett, J. Macnamara, P. Musch, J.M. Simmie, Simulation of methane autoignition in a rapid compression machine with creviced pistons, Combust. Flame 124 (2001) 326–329.
[11] V.P. Zhukov, V.A. Sechenov, A.Y. Starikovskii, Spontaneous ignition of methane–air mixtures in a wide range of pressures, Combust. Explos. Shock Waves 39 (2003) 487–495.
[12] J. Huang, P.G. Hill, W.K. Bushe, S.R. Munshi, Shock-tube study of methane ignition under engine-relevant conditions: experiments and modeling, Combust. Flame 136 (2004) 25–42.
[13] E.J. Hu, X.T. Li, X. Meng, Y.Z. Chen, Y. Cheng, Y.L. Xie, Z.H. Huang, Laminar flame speeds and ignition delay times of methane-air mixtures at elevated temperatures and pressures, Fuel 158 (2015) 1–10.
[14] H. El Merhubi, A. Keromnes, G. Catalano, B. Lefort, L. Le Moyne, A high pressure experimental and numerical study of methane ignition, Fuel 177 (2016) 164–172.
[15] H. Hashemi, J.M. Christensen, S. Gersen, H. Levinsky, S.J. Klippenstein, P. Glarborg, High-pressure oxidation of methane, Combust. Flame 172 (2016) 349–364.
[16] V.V. Leschevich, V.V. Martynenko, O.G. Penyazkov, K.L. Sevrouk, S.I. Shabunya, Auto-ignitions of a methane/air mixture at high and intermediate temperatures, Shock Waves 26 (2016) 657–672.
[17] A.C. Merkel, G. Ciccarelli, Visualization of lean methane-air ignition behind a reflected shock wave, Fuel 271 (2020) 117617.
[18] U. Burke, K.P. Somers, P. O'Toole, C.M. Zinner, N. Marquet, G. Bourque, E.L. Petersen, W.K. Metcalfe, Z. Serinyel, H.J. Curran, An ignition delay and kinetic modeling study of methane, dimethyl ether, and their mixtures at high pressures, Combust. Flame 162 (2015) 315–330.
[19] J.K. Shao, A.M. Ferris, R. Choudhary, S.J. Cassady, D.F. Davidson, R.K. Hanson, Shock-induced ignition and pyrolysis of high-pressure methane and natural gas mixtures, Combust. Flame 221 (2020) 364–370.
[20] G.P. Smith, D.M. Golden, M. Frenklach, N.W. Moriarty, B. Eiteneer, M. Goldenberg, C.T. Bowman, R.K. Hanson, S. Song, W.C. Gardiner Jr., GRI 3.0 mechanism. http://combustion.berkeley.edu/gri-mech/releases.html, 1999.
[21] M. Kelly, M. Fortune, G. Bourque, S. Dooley, Machine learned compact kinetic models for methane combustion, Combust. Flame 253 (2023) 112755.
[22] G. Smith, Y. Tao, H. Wang, Foundational fuel chemistry model version 1.0 (FFCM-1). http://nanoenergy.stanford.edu/ffcm1, 2016.
[23] J.C. Prince, F.A. Williams, Short chemical-kinetic mechanisms for low-temperature ignition of propane and ethane, Combust. Flame 159 (2012) 2336–2344.
[24] E. Ranzi, A. Frassoldati, R. Grana, A. Cuoci, T. Faravelli, A.P. Kelley, C.K. Law, Hierarchical and comparative kinetic modeling of laminar flame speeds of hydrocarbon and oxygenated fuels, Prog. Energy Combust. Sci. 38 (2012) 468–501.
[25] Y. Song, L. Marrodan, N. Vin, O. Herbinet, E. Assaf, C. Fittschen, A. Stagni, T. Faravelli, M.U. Alzueta, F. Battin-Leclerc, The sensitizing effects of NO2 and NO on methane low temperature oxidation in a jet stirred reactor, Proc. Combust. Inst. 37 (2019) 667–675.
[26] P. Glarborg, J.A. Miller, B. Ruscic, S.J. Klippenstein, Modeling nitrogen chemistry in combustion, Prog. Energy Combust. Sci. 67 (2018) 31–68.
[27] C.W. Zhou, Y. Li, U. Burke, C. Banyon, K.P. Somers, S.T. Ding, S. Khan, J.W. Hargis, T. Sikes, O. Mathieu, E.L. Petersen, M. AlAbbad, A. Farooq, Y.S. Pan, Y. J. Zhang, Z.H. Huang, J. Lopez, Z. Loparo, S.S. Vasu, H.J. Curran, An experimental and chemical kinetic modeling study of 1,3-butadiene combustion: ignition delay time and laminar flame speed measurements, Combust. Flame 197 (2018) 423–438.
[28] A.A. El-Sabor Mohamed, A.B. Sahu, S. Panigrahy, M. Baigmohammadi, G. Bourque, H. Curran, The effect of the addition of nitrogen oxides on the oxidation of propane: an experimental and modeling study, Combust. Flame 245 (2022) 112306.
[29] S. Panigrahy, J. Liang, M.K. Ghosh, Q.-D. Wang, Z. Zuo, S. Nagaraja, A.A.E.-S. Mohamed, G. Kim, S.S. Vasu, H.J. Curran, An experimental and detailed kinetic modeling study of the pyrolysis and oxidation of allene and propyne over a wide range of conditions, Combust. Flame 233 (2021) 111578.
[30] Z.-Y. Yang, P. Zeng, B.-Y. Wang, W. Jia, Z.-X. Xia, J. Liang, Q.-D. Wang, Ignition characteristics of an alternative kerosene from direct coal liquefaction and its blends with conventional RP-3 jet fuel, Fuel 291 (2021) 120258.
[31] J. Liang, C. Zhao, Z. Zhao, X. Wang, M.-X. Jia, Q.-D. Wang, Y. Zhang, F. Zhao, An experimental and kinetic modeling study on the high-temperature ignition and pyrolysis characteristics of cyclohexylamine, Combust. Flame 252 (2023) 112769.
[32] Q.-D. Wang, Y. Sun, Z. Zhao, Y. Zhang, F. Zhao, Y. Li, J. Liang, Ignition kinetics of nitrocyclohexane behind reflected shock waves in inert and air environments, Combust. Flame 255 (2023) 112865.
[33] A.G. Gaydon, I.R. Hurle, The Shock Tube in High-Temperature Chemical Physics, Reinhold Pub. Corp, 1963.
[34] M. Baigmohammadi, V. Patel, S. Nagaraja, A. Ramalingam, S. Martinez, S. Panigrahy, A.A.E.-S. Mohamed, K.P. Somers, U. Burke, K.A. Heufer, A. Pekalski, H. J. Curran, Comprehensive experimental and simulation study of the ignition delay time characteristics of binary blended methane, ethane, and ethylene over a wide range of temperature, pressure, equivalence ratio, and dilution, Energy Fuel. 34 (2020) 8808–8823.
[35] E.L. Petersen, M.J.A. Rickard, M.W. Crofton, E.D. Abbey, M.J. Traum, D.M. Kalitan, A facility for gas- and condensed-phase measurements behind shock waves, Meas. Sci. Technol. 16 (2005) 1716–1729.
[36] J. Guzman, G. Kukkadapu, K. Brezinsky, C. Westbrook, Experimental and modeling study of the pyrolysis and oxidation of an iso-paraffinic alcohol-to-jet fuel, Combust. Flame 201 (2019) 57–64.
[37] Y.P. Qu, C. Zou, W.X. Xia, Q.J. Lin, J.L. Yang, L.X. Lu, Y. Yu, Shock tube experiments and numerical study on ignition delay times of ethane in super lean and ultra-lean combustion, Combust. Flame 246 (2022).
[38] C.W. Zhou, Y. Li, E. O'Connor, K.P. Somers, S. Thion, C. Keesee, O. Mathieu, E.L. Petersen, T.A. DeVerter, M.A. Oehlschlaeger, G. Kukkadapu, C.J. Sung, M. Alrefae, F. Khaled, A. Farooq, P. Dirrenberger, P.A. Glaude, F. Battin-Leclerc, J. Santner, Y.G. Ju, T. Held, F.M. Haas, F.L. Dryer, H.J. Curran, A comprehensive experimental and modeling study of isobutene oxidation, Combust. Flame 167 (2016) 353–379.
[39] W. Xia, C. Peng, C. Zou, Y. Liu, L. Lu, J. Luo, Q. Lin, H. Shi, Shock tube and modeling study of ignition delay times of propane under O2/CO2/Ar atmosphere, Combust. Flame 220 (2020) 34–48.
[40] T. Lu, C.K. Law, Toward accommodating realistic fuel chemistry in large-scale computations, Prog. Energy Combust. Sci. 35 (2009) 192–215.
[41] Q.-D. Wang, Skeletal mechanism generation for methyl butanoate combustion via directed relation graph based methods, Acta Phys. Chim. Sin. 32 (2016) 595–604.
[42] Q.-D. Wang, S. Panigrahy, S. Yang, S. Martinez, J. Liang, H.J. Curran, Development of multipurpose skeletal core combustion chemical kinetic mechanisms, Energy Fuel. 35 (2021) 6921–6927.
[43] D.F. Davidson, R.K. Hanson, Recent advances in shock tube/laser diagnostic methods for improved chemical kinetics measurements, Shock Waves 19 (2009) 271–283.
[44] C.J. Sung, H.J. Curran, Using rapid compression machines for chemical kinetics studies, Prog. Energy Combust. Sci. 44 (2014) 1–18.

[45] D.G. Goodwin, R.L. Speth, H.K. Moffat, B.W. Weber, Cantera: an Object-Oriented Software Toolkit for Chemical Kinetics, Thermodynamics, and Transport Processes, 2018.
[46] J. Bugler, B. Marks, O. Mathieu, R. Archuleta, A. Camou, C. Gregoire, K.A. Heufer, E.L. Petersen, H.J. Curran, An ignition delay time and chemical kinetic modeling study of the pentane isomers, Combust. Flame 163 (2016) 138–156.
[47] S. Martinez, M. Baigmohammadi, V. Patel, S. Panigrahy, A.B. Sahu, S.S. Nagaraja, A. Ramalingam, A.A.S. Mohamed, K.P. Somers, K.A. Heufer, A. Pekalski, H. J. Curran, An experimental and kinetic modeling study of the ignition delay characteristics of binary blends of ethane/propane and ethylene/propane in multiple shock tubes and rapid compression machines over a wide range of temperature, pressure, equivalence ratio, and dilution, Combust. Flame 228 (2021) 401–414.
[48] A.B. Sahu, A.A. Mohamed, S. Panigrahy, C. Saggese, V. Patel, G. Bourque, W.J. Pitz, H.J. Curran, An experimental and kinetic modeling study of NOx sensitization on methane autoignition and oxidation, Combust. Flame 238 (2022).
[49] R. Zhu, C.C. Hsu, M.C. Lin, Ab initio study of the CH3+O2 reaction: kinetics, mechanism and product branching probabilities, J. Chem. Phys. 115 (2001) 195–203.
[50] F. Zhang, C. Huang, B. Xie, X. Wu, Revisiting the chemical kinetics of CH3 + O2 and its impact on methane ignition, Combust. Flame 200 (2019) 125–134.
[51] S. Sharma, S. Raman, W.H. Green, Intramolecular hydrogen migration in alkylperoxy and hydroperoxyalkylperoxy radicals: accurate treatment of hindered rotors, J. Phys. Chem. 114 (2010) 5689–5701.
[52] J.W. Sutherland, M.C. Su, J.V. Michael, Rate constants for H + CH_4, CH_3 + H_2, and CH_4 dissociation at high temperature, Int. J. Chem. Kinet. 33 (2001) 669–684.
[53] N.K. Srinivasan, M.C. Su, J.W. Sutherland, J.V. Michael, Reflected shock tube studies of high-temperature rate constants for CH_3 + O_2, H_2CO + O_2, and OH + O_2, J. Phys. Chem. 109 (2005) 7902–7914.
[54] N.K. Srinivasan, J.V. Michael, L.B. Harding, S.J. Klippenstein, Experimental and theoretical rate constants for CH_4 + O_2 → CH_3 + HO_2, Combust. Flame 149 (2007) 104–111.
[55] R.S. Zhu, M.C. Lin, The CH_3 + HO_2 reaction: first-principles prediction of its rate constant and product branching probabilities, J. Phys. Chem. A 105 (2001) 6243–6248.
[56] A.W. Jasper, S.J. Klippenstein, L.B. Harding, Theoretical rate coefficients for the reaction of methyl radical with hydroperoxyl radical and for methylhydroperoxide decomposition, Proc. Combust. Inst. 32 (2009) 279–286.
[57] Z.K. Hong, D.F. Davidson, K.Y. Lam, R.K. Hanson, A shock tube study of the rate constants of HO_2 and CH_3 reactions, Combust. Flame 159 (2012) 3007–3013.
[58] T.A. Kashif, M. AlAbbad, M. Figueroa-Labastida, O. Chatakonda, J. Kloosterman, J. Middaugh, S.M. Sarathy, A. Farooq, Effect of oxygen enrichment on methane ignition, Combust. Flame 258 (2023) 113073.